
Supplementary information

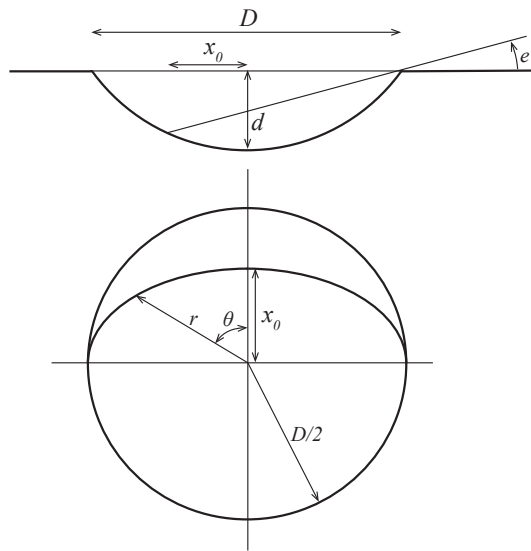
Micro cold traps on the Moon

In the format provided by the
authors and unedited

Supplementary Material for
Micro cold traps on the Moon

P. O. Hayne¹ O. Aharonson^{2,3} N. Schörghofer^{3,4}

Supplementary Figures



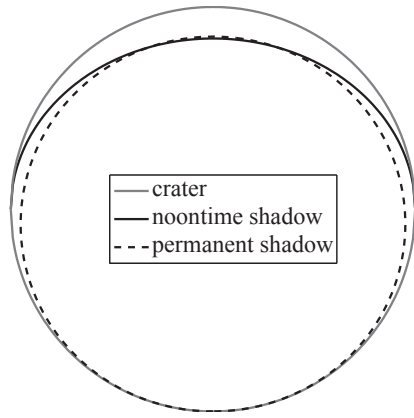
Supplementary Figure 1: Vertical and horizontal cross sections of spherical crater with shadow, with definitions for variables.

¹Laboratory for Atmospheric & Space Physics, and Astrophysical & Planetary Sciences Department, University of Colorado Boulder, Colorado, USA. Paul.Hayne@Colorado.edu

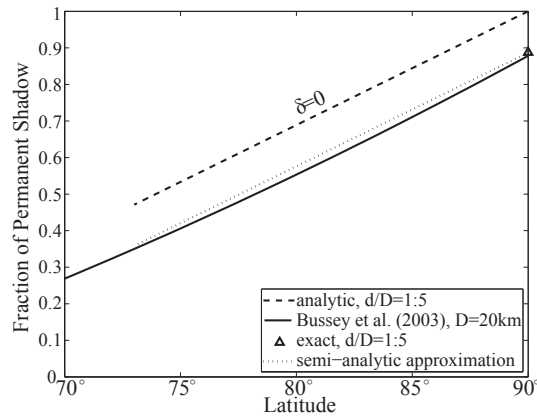
²Helen Kimmel Center for Planetary Science, Weizmann Institute of Science, Rehovot, Israel.

³Planetary Science Institute, Tucson, Arizona, USA.

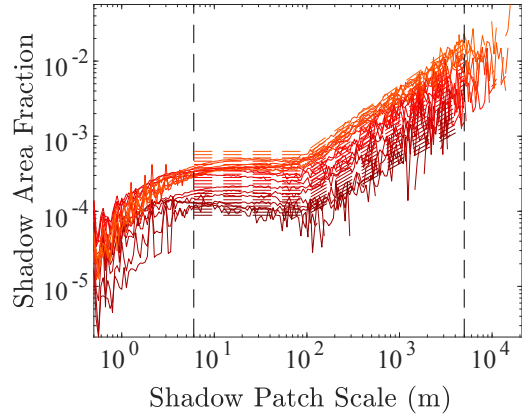
⁴Planetary Science Institute, Honolulu, Hawaii, USA



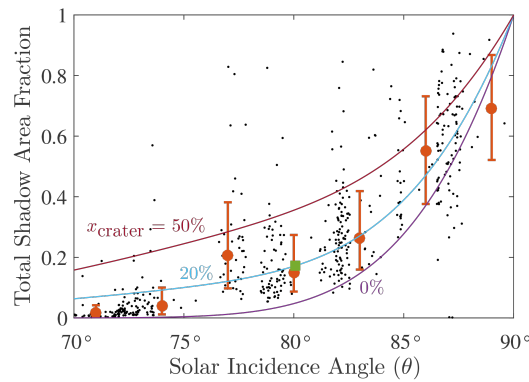
Supplementary Figure 2: Top view of circular crater with the exact noontime shadow boundary and the approximate extent of permanent shadow. The diameter to depth ratio of the crater is 5 and the maximum elevation of the Sun, e_0 , is 4° .



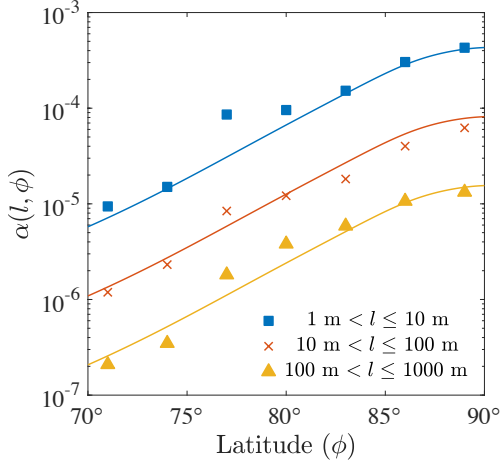
Supplementary Figure 3: Comparison between the numerical results of Bussey et al.¹, the analytic result for zero declination (??), and approximation (??). The triangle shows the analytic result for the pole (??).



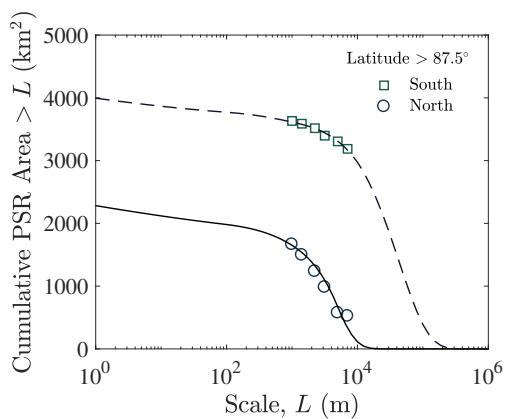
Supplementary Figure 4: Instantaneous shadow fraction from LROC-NAC images for a range of solar incidence angles (68° , 69° , ..., 88° , lighter tones representing increasing incidence angle), binned in logarithmically spaced shadow patch scales from 0.5 m to 50 km. Dashed lines represent a fit to the data.



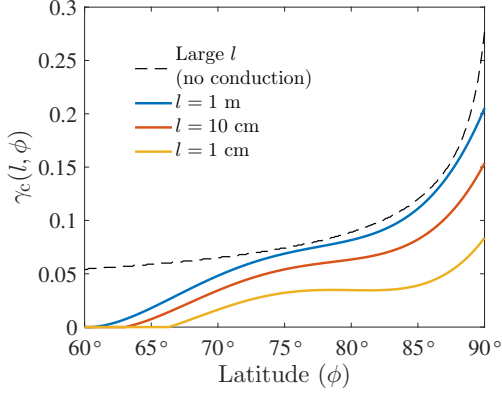
Supplementary Figure 5: Comparison of shadow fraction from LROC image data (points) to the model (curves). Error bars indicate the mean and standard deviations within each solar incidence angle bin, and x_{crater} is the area occupied by craters within the rough terrain.



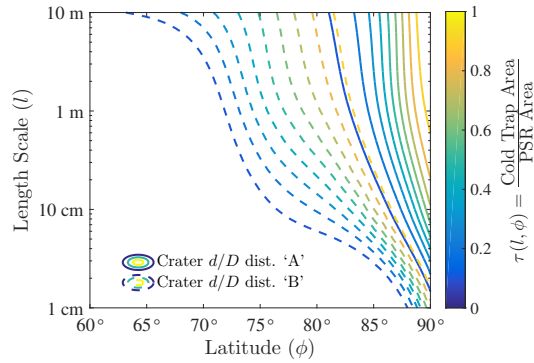
Supplementary Figure 6: Fraction α (units of m^{-1}) of the total surface area occupied by permanent shadows as a function of latitude φ and length scale l . The model curves shown assume a crater fraction of 20% and inter-crater plains with RMS slope $\sigma_s = 5.7^\circ$



Supplementary Figure 7: Cumulative fraction of the total surface area occupied by permanent shadows with length scale $l > L$. Data points are from Mazarico et al.², for each polar region, $> 87.5^\circ$.

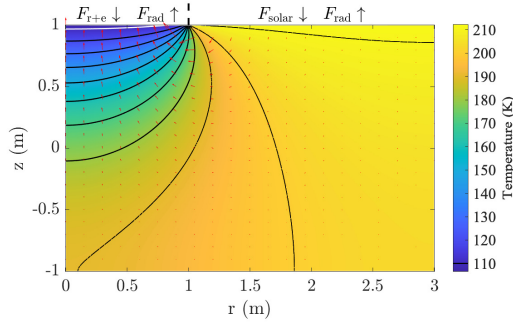


Supplementary Figure 8: Critical depth/diameter ratio γ_c of craters, for which $\gamma < \gamma_c$ indicates the PSR is a cold trap for water ice.

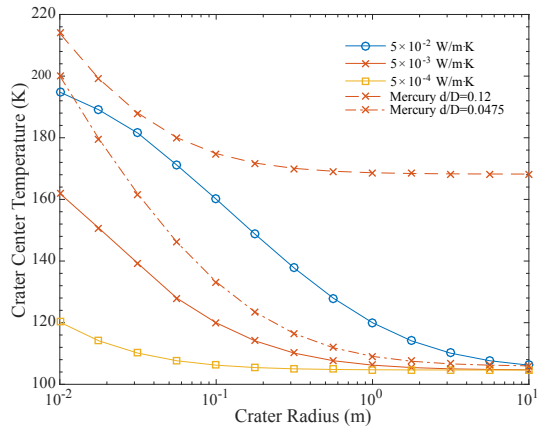


Supplementary Figure 9: Fraction of permanently shadowed regions (PSR) inside craters that are cold traps for water ice, $T_{\max} < 110$ K. Results are shown for two log-normal probability distributions ‘A’ (deeper craters, $\mu = 0.14$) and ‘B’ (shallower craters, $\mu = 0.076$). Contours are plotted for $\tau = 0.1, 0.2, \dots, 0.9$.

a)



b)



Supplementary Figure 10: Solution to the heat equation in a cylindrically symmetric geometry. a) Cross section through the domain showing temperature contours and heat flow directions. b) Temperature at the center of a crater (representing the minimum temperature) for different thermal and orbital assumptions.

References

- [1] Bussey, D. B. J. *et al.* Permanent shadow in simple craters near the lunar poles. *Geophys. Res. Lett.* **30**, 1278 (2003).
- [2] Mazarico, E., Neumann, G. A., Smith, D. E., Zuber, M. T. & Torrence, M. H. Illumination conditions of the lunar polar regions using LOLA topography. *Icarus* **211**, 1066–1081 (2011).